

Pressure-induced metallization and collapse of the antiferromagnetic state of MnTe₂

P. Vulliet,^{1,2} J. P. Sanchez,^{1,*} D. Braithwaite,¹ M. Amanowicz,¹ and B. Malaman³

¹*Département de Recherche Fondamentale sur la Matière Condensée, SPMS, CEA-Grenoble, 17 rue des Martyrs, 38054 Grenoble Cedex 9, France*

²*Université Joseph Fourier, Boîte Postale 53, 38041 Grenoble Cedex 9, France*

³*Laboratoire de Chimie du Solide Minéral, Associé au CNRS (UMR7555), Université Henri Poincaré-Nancy I, Boîte Postale 239, 54506 Vandoeuvre les Nancy Cedex, France*

(Received 7 December 2000; published 12 April 2001)

The electronic ground state and structural and magnetic properties of the pyrite-type antiferromagnetic semiconductor MnTe₂ have been investigated by combining ¹²⁵Te Mössbauer spectroscopy and x-ray-diffraction and electrical resistance measurements at pressures up to 22.5 GPa and temperatures of 4.2–300 K. It was shown that the first-order phase transition towards a denser high-pressure pyrite phase, taking place at ≈8 GPa (increasing pressure), is accompanied by an insulator-metal transition leading to a nonmagnetic Mn²⁺ ground state.

DOI: 10.1103/PhysRevB.63.184403

PACS number(s): 75.30.Kz, 71.30.+h, 76.80.+y

I. INTRODUCTION

The discovery of high- T_C superconducting cuprates and the giant magnetoresistance effects in La manganites has initiated a renewed interest in the study of the electronic and magnetic properties of 3d transition-metal compounds, and a major issue is understanding the metal-insulator (MI) transition. This is because many of the 3d compounds (oxides, halides, and chalcogenides) are antiferromagnetic (AF) insulators at low temperatures, and their properties are drastically altered by varying either composition of the cation/anion sublattices or by applying pressure or changing the temperature.¹ A spectacular example of the consequence of pressure is NiI₂, which undergoes a pressure-induced transition from an AF insulating state to a nonmagnetic metallic state without changing the crystal structure.² This type of transition is of special interest because its pure electronic nature is of importance for understanding the broad class of strongly correlated systems.

The qualitative behavior of the MI transition in such systems has been understood for a long time using the Mott-Hubbard theory.^{1,3,4} However details of this theory were in disagreement with experiments. It does not explain, for instance, why NiO and CoO are insulators but NiS, CuS, and CoS are metals or why the optical band gap in the Ni dihalides depends on the anion electronegativity. It is now well documented^{5–7} that the 3d compounds can, in fact, be classified into two regimes, i.e., the insulating gap may be either of the Mott-Hubbard type or of the charge-transfer type, depending on the relative magnitude of the intra-atomic Coulomb energy (U) that splits the d band, and the charge-transfer energy (Δ), which corresponds to the excitation of an electron from the anion valence band to the transition-metal ion. Thus according to Zaanen, Sawatsky, and Allen⁵ for $U < \Delta$, the system is in the Mott-Hubbard regime with a d - d gap for $U > W$ and a d metal for $U < W$ (W being the d -band dispersional energy). By contrast, for $U > \Delta$ the gap is of the charge-transfer type and if $\Delta < W$ the ground state is a p metal (W being the p -band dispersional energy). The early transition-metal compounds belong in general to the Mott-

Hubbard regime whereas the later transition-metal compounds fall into the charge-transfer regime. NiI₂, mentioned above, should be classified as a charge-transfer insulator. Indeed, resistivity and near-ir absorption measurements on NiI₂ under pressure suggest that closure of the charge-transfer energy gap is the fundamental cause of the observed MI transition.⁸

Divalent manganese compounds stand apart because of the large stabilization of the 3d⁵ high-spin ground state. This causes Δ and U to be of comparable magnitude and larger than those of neighboring 3d metal ion compounds of a given series.⁶ This explains why MnTe₂ is nonmetallic while CoTe₂ and NiTe₂ are metals at ambient conditions.⁹ Furthermore it is expected that in the Mn²⁺ compounds, hole and electron mobilities are similar.

This work reports on the high-pressure behavior of MnTe₂ using the combined methods of ¹²⁵Te Mössbauer spectroscopy, energy-dispersive x-ray diffraction, and electrical conductivity. The compound under study is known to be a semiconductor^{9,10} that crystallizes with the pyrite structure (space group $Pa\bar{3}$). Recent photoemission spectroscopy measurements and comparisons with local spin density and configuration-interaction calculations allow us to classify MnTe₂ as a charge-transfer insulator ($\Delta = 1.5$, $U = 5.5$ eV) and the value of the ligand p -metal d hybridization energy ($T = 1.4$ eV) confirms the $p \rightarrow d$ charge-transfer nature of the band gap.¹¹ MnTe₂ undergoes a second-order antiferromagnetic transition at $T_N \approx 86.5$ K. The nature of its magnetic structure, which has been subject to controversy, was recently shown to be noncollinear with the magnetic moments ($4.28\mu_B$) of the four Mn²⁺ ions of the unit cell pointing along different body diagonals of the cube ($\mu_{Mn} // \langle 111 \rangle$).¹² The occurrence of strong covalency effects, i.e., electron transfer between the ligands and the Mn²⁺ ions, was concluded from the observation of a spin density at the tellurium site and from the significant reduction of both the quadrupolar interaction (Te) and the ordered Mn moment as compared to the values expected for the free Te₂²⁻ and Mn²⁺ ions.¹² The effect of applied pressure on the structural properties of

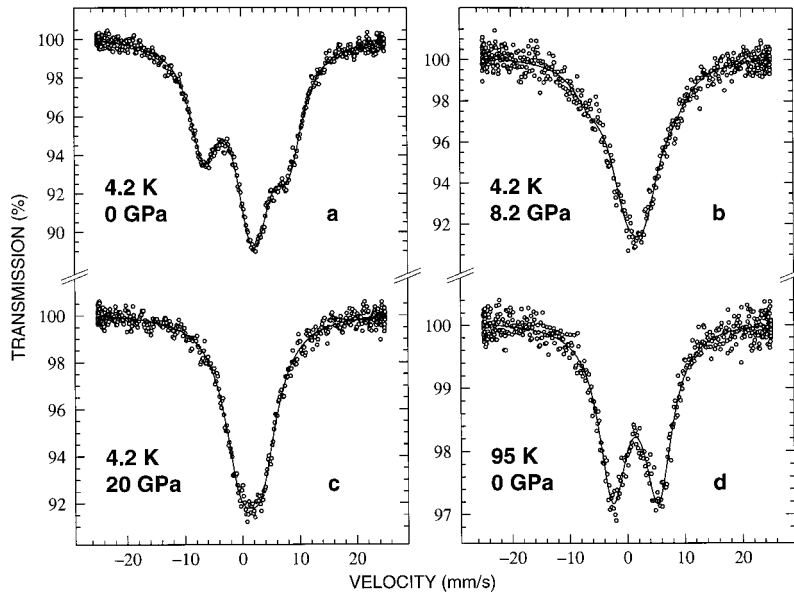


FIG. 1. Typical ^{125}Te Mössbauer spectra of MnTe_2 at 4.2 K and 0, 8.2, and 20 GPa and at 95 K and ambient pressure. The solid line is the result of a least-squares fit of the data. (a) Low-pressure pyrite phase (magnetic state), (b) coexistence of the low-pressure pyrite phase (magnetic) with the high-pressure pyrite phase (nonmagnetic), (c) high-pressure pyrite phase (nonmagnetic), and (d) low-pressure pyrite phase (paramagnetic state).

MnTe_2 was already considered by Fjellvåg *et al.*^{13,14} who first used a conventional x-ray source and later synchrotron radiation. They concluded that the pressure-induced structural change at ≈ 8 GPa is strongly affected by the hydrostaticity conditions. The observed high-pressure phases were of the pyrite or/and marcasite type(s). The first-order transition accompanied by a large volume reduction ($\approx 16\%$) was attributed to changes in the electronic properties.¹⁴ The aim of our work was to elucidate the nature of this pressure-induced electronic transition.

II. EXPERIMENTAL PROCEDURE

A. Sample preparation

MnTe_2 was prepared from stoichiometric amounts of Mn (99.9%) and 15% ^{125}Te enriched elemental tellurium. The pellet made of the starting materials was heated in a silica tube under argon (300-mm Hg) first at 773 K for a preliminary homogenization and then at 873 K for 2 weeks. Powder x-ray diffraction showed that the final product is single phase with a pyrite-type structure. Samples for resistance measurements were tiny single crystals obtained by the “flux-growth” method described previously.¹²

B. High-pressure ^{125}Te Mössbauer methodology

^{125}Te -Mössbauer-spectroscopy pressure studies were performed over extended temperature (4.2–300 K) and pressure ranges (up to 22.5 GPa). The enriched MnTe_2 sample was loaded in a miniature diamond-anvil cell (DAC) using a 50- μm -thick $\text{Ta}_{0.9}\text{W}_{0.1}$ gasket with a drilled hole of 250 μm . An external Ta collimator was placed as close as possible to the entrance diamond to avoid transmission of the 35.5-keV γ rays through the gasket. Argon was used as the pressure medium. The pressure was measured at room temperature with the ruby fluorescence method. Uncertainties in pressure did not exceed 0.3 GPa.

The Mössbauer spectra were obtained using a small-size (2-mm diameter) neutron-activated $\text{Mg}_3^{125}\text{TeO}_6$ source kept either at 4.2 or 77 K. The 35.5-keV γ rays were counted with an intrinsic Ge detector and typical count rates through the DAC were about 50 counts/s and typically data for each pressure were accumulated for a period of 2–3 days. In the case of combined quadrupole and magnetic interactions, the experimental data were computer analyzed by diagonalization of the full nuclear Hamiltonian.

C. Energy-dispersive x-ray diffraction (EDXR)

The experiments were carried out at room temperature at the energy-dispersive x-ray (EDX) station of LURE (DCI Orsay) using the Mössbauer DAC loaded at a pressure of 18 GPa. The diffraction data were collected at three different scattering angles of 6.50° , 7.27° , and 8.10° because the observation of the Bragg reflections of the high-pressure phase was hampered by the $K_{\alpha 1,2}$ and $K_{\beta 1,2}$ characteristic lines of Te (27.47, 27.20 and 31.0, 31.7 keV, respectively).

D. High-pressure resistance measurements

The measurements were carried out in a Bridgman-type sintered diamond-anvil cell with steatite as the pressure-transmitting medium. The pressure was changed at room temperature and measured at low temperature using the superconducting transition of lead. The samples were single crystals of MnTe_2 . All “large” crystals having sizes of about $500 \times 200 \times 50 \mu\text{m}^3$ proved too fragile and broke on application of pressure. A successful loading was eventually made with a sample with dimensions of about $150 \times 100 \times 30 \mu\text{m}^3$. The electrical contacts were made with 10- μm gold wire instead of the normal 25- μm platinum wire. Because of these difficulties some contacts proved temperamental, causing some extra noise and missing data regions. They also prevented us from measuring the pressure accurately for the first three pressure steps. A successful experiment was nevertheless carried out up to 18.8 GPa. The missing pres-

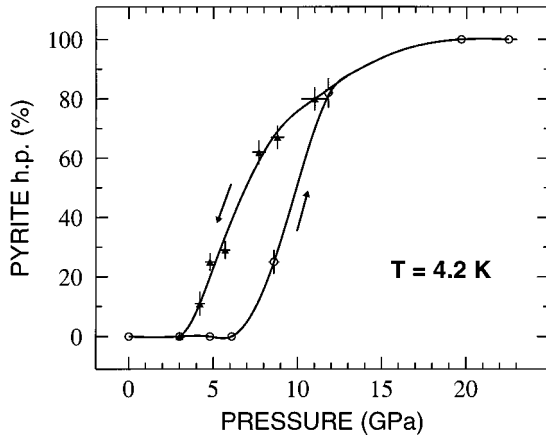


FIG. 2. Pressure dependence of the relative abundance of the high-pressure pyrite phase at 4.2 K as deduced from the Mössbauer data; increasing pressure (○), decreasing pressure (▲).

sure values can be deduced from the applied force and the sample data, notably the pressure dependence of T_N .

III. RESULTS AND DISCUSSION

Typical ^{125}Te Mössbauer spectra recorded at different pressures and temperatures are shown in Fig. 1. In the first pressure regime up to $P_c \approx 8$ GPa, the 4.2 K spectra are characteristic of a single magnetic component. Their spectral shape is interpreted by diagonalization of a hyperfine interaction Hamiltonian involving both a transferred hyperfine field $H_{\text{hf}}^{\text{tr}}$ and a quadrupole splitting $QS = 1/2e^2q_{zz}Q$.¹² It was found that $H_{\text{hf}}^{\text{tr}}$ (essentially a measure of the spin density in the ^{125}Te 5s orbital), QS (due to the ^{125}Te 5p-electron imbalance), and θ (the angle between the principal axis of the electric-field gradient eq_{zz} and $H_{\text{hf}}^{\text{tr}}$) remain constant up to P_c ($H_{\text{hf}}^{\text{tr}} \approx 97$ kG, $e^2q_{zz}Q \approx -8$ mm/s, $\theta \approx 16^\circ$).^{12,15,16} With increasing pressure in the range of 8–15 GPa, a nonmagnetic component evolves. This component coexists with the original low-pressure magnetic phase. The pressure dependence of the relative abundance of the nonmagnetic component as derived from the analysis of the Mössbauer spectra is shown in Fig. 2. In the pressure regime above 15 GPa, the spectra are satisfactorily fitted with a single nonresolved quadrupole doublet ($QS \approx 3.5$ mm/s at 20 GPa and 4.2 K) which is similar to the one observed in metallic nonmagnetic FeTe_2 or CoTe_2 compounds.¹⁷

The observed behavior leads us to conclude that both the Mn moment and the noncollinear magnetic structure of MnTe_2 remain stable in the low-pressure pyrite phase. The variation of its ordering temperature T_N with pressure as deduced from the (P, T) dependence of the Mössbauer spectra is shown in Fig. 3. As can be seen, T_N increases by a factor of ≈ 2 from 86.5 K at 0 GPa to 179 K at 7.2 GPa. The linear increase of T_N at a rate of ≈ 12 K GPa^{-1} simply reflects the increase of the exchange integrals with decreasing volume.²

The Mössbauer data fully agree with the first-order nature of the phase transition and the stability range of the low-pressure pyrite phase observed previously by x-ray diffraction.¹⁴ As we used nearly hydrostatic conditions, the high-

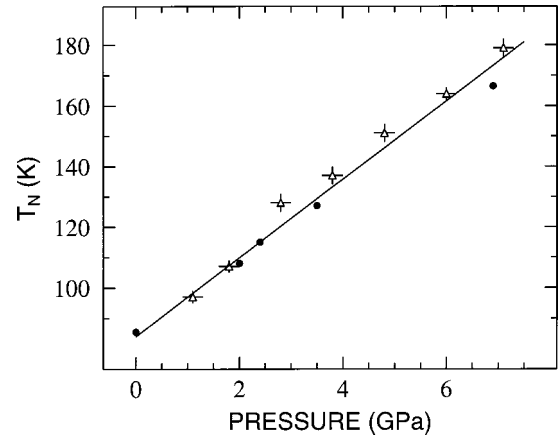


FIG. 3. Néel temperature T_N of the low-pressure pyrite phase as a function of pressure as derived from the Mössbauer (Δ) and resistance (\bullet) data. The straight line is a fit through the experimental data.

pressure phase was expected, according to Ref. 14, to be of pyrite type. That was nicely confirmed from our EDXR experiment performed at 18 GPa (Fig. 4). The low-pressure (LP) and high-pressure (HP) pyrite phases coexist in the pressure range 9–15 GPa on increasing pressure and 15–4 GPa on decreasing pressure (Fig. 2).

The observation that the HP pyrite phase exhibits only an unresolved quadrupole splitting down to 4.2 K suggests that the Mn ions are not in a paramagnetic configuration, i.e., the phase transition does not involve a change of the crystal-field splitting and an accompanying high-spin ($S = \frac{5}{2}$) \rightarrow low-spin ($S = \frac{1}{2}$) crossover of the Mn^{2+} ions. Alternatively, the lack of magnetic order could indicate the breakdown of the d - d electronic correlation and a concomitant metallization of MnTe_2 . Our high-pressure resistance measurements, as shown below, indicate that the latter scenario takes place in MnTe_2 .

The temperature dependence of the resistance at various pressures is shown in Figs. 5(a) and (b). As can be seen the

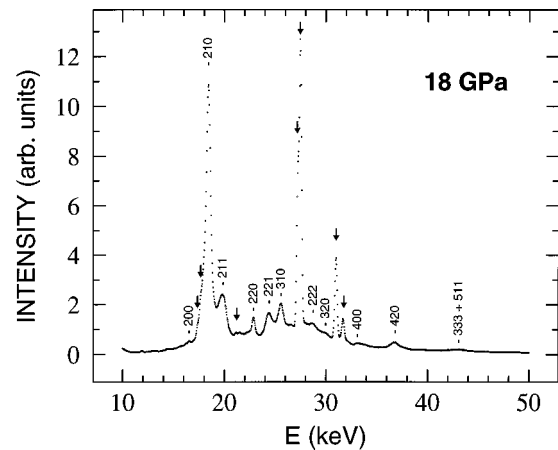


FIG. 4. Energy-dispersive x-ray-diffraction pattern of the high-pressure pyrite-type phase of MnTe_2 collected at a scattering angle of $\theta = 7.27^\circ$ at RT and 18 GPa. Indexing of the diffraction lines given on the figure leads to $a = 5.95(5)$ Å. The arrows indicate the positions of the escape lines and of the K_α , K_β Te lines.

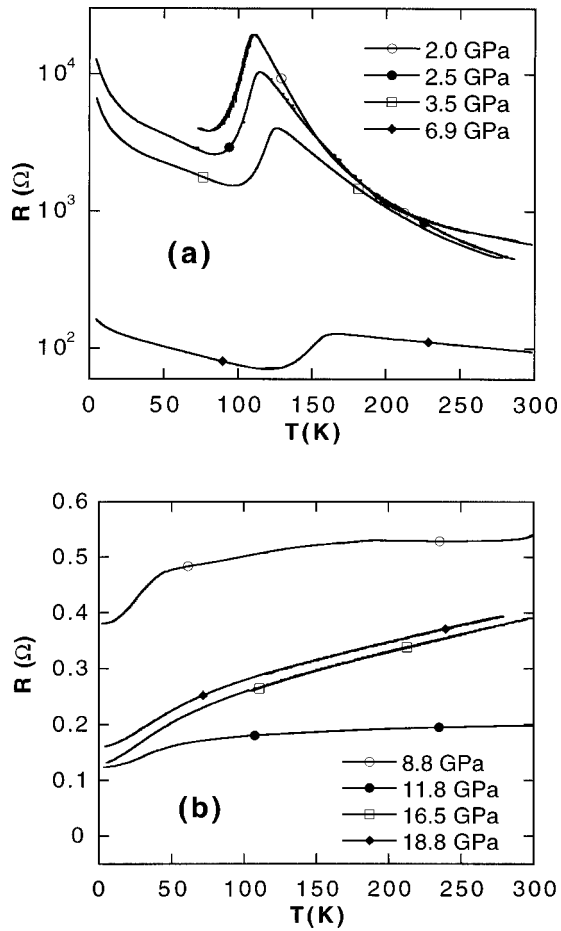


FIG. 5. (a) Temperature dependence at various pressures of the resistance of the low-pressure pyrite phase of MnTe_2 . Note the semiconductorlike behavior and the steep increase of T_N with increasing pressure. (b) Temperature dependence of the resistance of MnTe_2 at pressures above the critical pressure for the onset of the insulator-metal transition. The shape of the (R, T) curve at 8.8 GPa suggests the coexistence of the insulating low-pressure pyrite phase with the metallic high-pressure pyrite phase. The curves at higher pressures indicate pure metallic behavior.

distinctive feature, found from previous zero-pressure experiments to correspond to the Néel temperature, is clearly visible in the low-pressure regime [Fig. 5(a)]. In fact, it is more pronounced than in previously published measurements.¹⁸ The Néel temperature in these crystals was checked at zero pressure with a superconducting quantum interference device magnetometer and found to be around 85 K in agreement with previous results.¹² From the resistance data T_N is found to increase to 166 K at 6.9 GPa. This fits well with the Mössbauer results (Fig. 3) but disagrees with another high-pressure resistance study.¹⁹

Between 7–9 GPa, an insulator-to-metal transition is found [Figs. 5(a) and (b)] that corresponds to the structural phase transition. In the LP-pyrite phase the effect of pressure is to gradually decrease the resistance while keeping a semiconductorlike behavior. The effect on the transition to the high-pressure phase is quite brutal and the resistance decreases by a factor of 500 (Fig. 6). The relatively high resistance at 8.8 GPa and the slightly “bumpy” nature of the

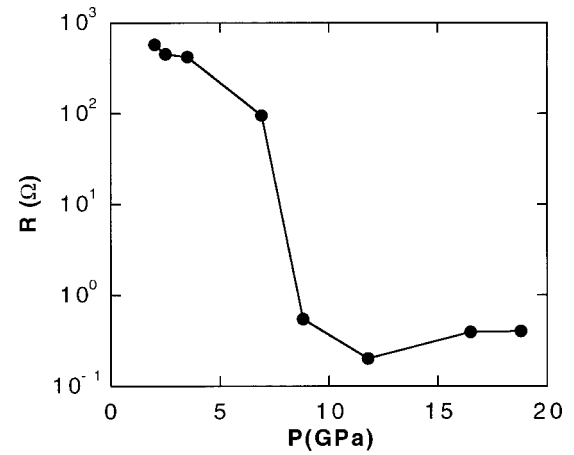


FIG. 6. Pressure dependence of the resistance at 300 K. Note the large decrease in R around 8 GPa indicating the metallization of MnTe_2 .

curve is probably due to a proportion of the LP-pyrite phase still present. At higher pressures the $R(P, T)$ curves look as though we have the pure high-pressure phase. As pressure is increased the curves become more metallic in nature, but surprisingly the high-temperature resistance level increases [Fig. 5(b)].

The measurements made while decreasing pressure are, as usual, far less reliable. They seem to show that there is a large hysteresis in the phase transition, in agreement with the Mössbauer data (Fig. 2). Although the low-pressure phase starts to appear around 8 GPa, some of the high-pressure phase is probably maintained down to zero pressure.

In conclusion, the present study clarifies the nature of the high-pressure structural and electronic states of MnTe_2 . Upon increasing pressure a first-order phase transition towards a denser (16% collapse in volume) pyrite phase occurs around 8 GPa. The isostructural phase transition is accompanied by a metallization of MnTe_2 whose ground state is non-magnetic. It is suggested that the pressure-induced metallization and collapse of the Mn moment is due to the closure of the p - d charge-transfer gap (Δ). It may be anticipated that a similar situation to that of MnTe_2 exists for the isostructural MnS_2 and MnSe_2 . High-pressure Mössbauer data for ^{57}Fe substitution in MnX_2 ($X = \text{S}, \text{Se}, \text{and Te}$) support this assumption.²⁰ The higher critical pressure (≈ 14 GPa) found for MnS_2 (Ref. 21) is in line with the expected increase of Δ with the ionicity of the Mn^{2+} - X_2^{2-} bonds. We feel that our results would stimulate further experimental and theoretical efforts for a better understanding of the pressure-induced structural, electronic, and magnetic phenomena in the MnX_2 series. Future experimental works should be devoted to a direct determination of the gap closure by optical methods as well as to the pressure dependence of the Mn moment by new tools such as the resonant x-ray magnetic-diffraction technique.²²

ACKNOWLEDGMENTS

Thanks are due to J. P. Itié and A. Polian for their help during the EDXR measurements.

*Corresponding author.

- ¹N. F. Mott, *Metal-Insulator Transitions* (Taylor & Francis, London, 1990).
- ²M. P. Pasternak, R. D. Taylor, A. Chen, C. Meade, L. M. Falicov, A. Giesekus, R. Jeanloz, and P. Y. Yu, Phys. Rev. Lett. **65**, 790 (1990).
- ³N. F. Mott, Proc. Phys. Soc., London, Sect. A **62**, 416 (1949).
- ⁴J. Hubbard, Proc. R. Soc. London, Ser. A **277**, 237 (1964); **281**, 401 (1964).
- ⁵J. Zaanen, G. A. Sawatzky, and J. W. Allen, Phys. Rev. Lett. **55**, 418 (1984).
- ⁶J. Zaanen and G. A. Sawatzky, Can. J. Phys. **65**, 1262 (1987); J. Solid State Chem. **88**, 8 (1990).
- ⁷M. Imada, A. Fujimori, and Y. Tokura, Rev. Mod. Phys. **70**, 1039 (1998).
- ⁸A. L. Chen, P. Y. Yu, and R. D. Taylor, Phys. Rev. Lett. **71**, 4011 (1993).
- ⁹G. Brostigen and A. Kjekshus, Acta Chem. Scand. **24**, 2993 (1970).
- ¹⁰N. Kasai, S. Waki, and S. Ogawa, J. Phys. Soc. Jpn. **50**, 3303 (1981).
- ¹¹K. V. Kaznacheev, T. Muro, T. Matsushita, T. Iwasaki, Y. Kuwata, H. Harada, S. Suga, H. Ishii, T. Miyahara, T. Mizokawa, A. Fujimori, T. Harada, and T. Kanomata, Phys. Rev. B **58**, 13 491 (1998).
- ¹²P. Burllet, E. Ressouche, B. Malaman, R. Welter, J. P. Sanchez, and P. Vulliet, Phys. Rev. B **56**, 14 013 (1997), and references therein.
- ¹³H. Fjellvåg, A. Kjekshus, T. Chattopadhyay, H. D. Hochheimer, W. Hönle, and H. G. von Schnering, Phys. Lett. **112A**, 111 (1985).
- ¹⁴H. Fjellvåg, W. A. Grosshans, W. Hönle, and A. Kjekshus, J. Magn. Magn. Mater. **145**, 118 (1995).
- ¹⁵M. P. Pasternak and R. D. Taylor, in *Mössbauer Spectroscopy Applied to Magnetism and Materials Science*, edited by G. J. Long and F. Grandjean (Plenum, New York, 1996), Vol. 2, p. 167.
- ¹⁶P. Vulliet, J. P. Sanchez, J. Thomasson, B. Malaman, and R. Welter, in *Proceedings of the ICAME, Rimini, Italy, 1995*, edited by I. Ortalli (Societa Italiana di Fisica, Bologna, 1996), Vol. 50, p. 231.
- ¹⁷J. Stanek, A. M. Khasanov, and S. S. Hafner, Phys. Rev. B **45**, 56 (1992).
- ¹⁸A. Sawaoka and S. Miyahara, J. Phys. Soc. Jpn. **20**, 2087 (1965).
- ¹⁹A. Sawaoka, S. Miyahara, and S. Minomura, J. Phys. Soc. Jpn. **21**, 1047 (1966).
- ²⁰C. B. Barger, M. Avinor, and H. G. Drickamer, Inorg. Chem. **10**, 1338 (1971).
- ²¹T. Chattopadhyay and H. von Schnering, J. Phys. Chem. Solids **46**, 113 (1985).
- ²²J. P. Hannon, G. T. Trammel, M. Blume, and D. Gibbs, Phys. Rev. Lett. **61**, 1241 (1988).